Formation and Thickness Evolution of Periodic Twin Domains in Manganite Films Grown on $SrTiO_3(001)$ Substrates

U. Gebhardt,[1] N. V. Kasper,[1] A. Vigliante,[1,*] P. Wochner,[1] H. Dosch,[1] F. S. Razavi,[2,†] and H.-U. Habermeier[2]

[1]*Max-Planck-Institut für Metallforschung, Heisenbergstraße 3, 70569 Stuttgart, Germany*

[2]*Max-Planck-Institut für Festkörperforschung, Heisenbergstraße 1, 70569 Stuttgart, Germany*

(Received 17 February 2006; published 27 February 2007)

We present an extended synchrotron x-ray scattering study of the structure of thin manganite films grown on $SrTiO_3(001)$ substrates and reveal a new kind of misfit strain relaxation process which exploits twinning to adjust lattice mismatch. We show that this relaxation mechanism emerges in thin films as one-dimensional twinning waves which freeze out into a twin domain pattern as the manganite film continues to grow. A quantitative microscopic model which uses a matrix formalism is able to reproduce all x-ray features and provides a detailed insight into this novel relaxation mechanism. We further demonstrate how this twin angle pattern affects the transport properties in these functional films.

DOI: 10.1103/PhysRevLett.98.096101 PACS numbers: 68.55.−a, 61.10.Eq, 71.27.+a, 71.30.+h

Since the discovery of colossal magnetoresistance (CMR) in perovskite type $(Ln_{1-\delta}A_\delta)MnO_3$ (Ln = lanthanides, A = alkaline earth elements) there has been enormous interest in these materials both in bulk and thin-film form because of their unusual physical properties, such as the metal-insulator phenomena or the cooperative ordering of orbital, charge, and spin, and because of their potential applications such as magnetic field sensors, computer read heads, infrared detectors, and microwave active components.

In bulk manganese oxides the transport properties depend on band filling (doping degree), temperature, magnetic field, and eventually present lattice distortions [1]. Since future applications will extensively exploit thin-film geometries, the associated transport properties will strongly be determined by the strain misfit as caused by the microscopic clamping of the film to the substrate. A striking example hereof are Sr doped lanthanum manganite films (denoted as LSMO) ($\delta = 0.10$, $t \leq 50$ nm) grown on a $SrTiO_3(001)$ substrate (denoted as STO), which show metallic behavior at low temperatures instead of the expected insulating bulk behavior [2].

While conventional film material adjusts its lattice parameters to the substrate by stretching or compressing its bond lengths, thereby paying a high energy penalty, a perovskite film may use tilting of its oxygen octahedra for strain accommodation at relatively low energy costs (see Fig. 1) [3]. Single crystals are naturally microtwinned indicating a low energy cost for domain boundaries [4]. Exploiting both aspects, manganite films are able to grow epitaxially on a perovskite substrate even for large lattice misfits. Note that, according to the double-exchange model [5], the electron hopping probability (i.e., the electron transport) in such systems depends sensitively on the Mn-O-Mn bond angle. Thus, by a microscopic understanding of this misfit strain relaxation mechanism one may get a tool at hand for tuning the electronic properties of manganite films.

In this Letter we present a systematic x-ray study of the strain relaxation behavior of LSMO films on STO substrates with compositions of $La_{0.88}Sr_{0.10}MnO_3$, $La_{0.90}Sr_{0.10}MnO_3$, or $La_{0.875}Sr_{0.125}MnO_3$ and with film thicknesses varying from 12 to 110 nm. We will show that the strained films exhibit an intriguing strain accommodation scenario: they first develop periodic 1-dimensional (1D) twinning modulation waves which progressively develop into a twin domain (TD) pattern as the film thickness increases.

LSMO films of different thicknesses have been grown on STO(001) by using pulsed laser deposition [2,6]. Subsequent *in situ* 1 atm oxygen annealing at 900 °C for 1 h leads to a homogenous oxygen stoichiometry throughout the film. At room temperature (RT), the film-substrate lattice mismatch $\epsilon = (a_{LSMO} - a_S)/a_S$ extends from -0.45% ($La_{0.88}Sr_{0.10}MnO_3$) to $+0.95\%$ ($\delta = 0.10$) and $+0.23\%$ ($\delta = 0.125$) [7–10]. The lattice miscut angle $\alpha < 0.35°$ for all investigated samples and the miscut direction covers the range of $-63° \leq \beta \leq 69°$ with respect to [100]/[010]. Although bulk LSMO has a lower symmetry

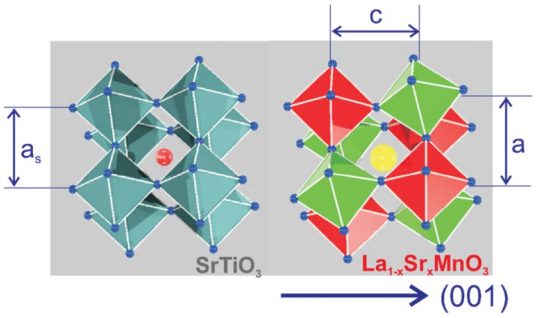

FIG. 1 (color). Sketch of the triclinic structure of the LSMO film and the cubic structure of the STO substrate at RT. The oxygen octahedras and the A-site cations (La,Sr) are shown. The B-site cations (Mn,Ti) are positioned in the center of the octahedras.

than STO [11] the average structure of all investigated LSMO films is pseudomorphic with respect to the STO substrate, leading to a triclinic distortion of $F\bar{1}$ symmetry (see also [12]). In what follows, the cubic coordinates in real space are specified as x, y, and z, the ones in reciprocal space as ξ, η, and ζ corresponding to the Miller indices H, K, and L. The reciprocal lattice units (denoted as r.l.u.) are based on the STO substrate ($a_S = 3.905$ Å).

The synchrotron x-ray diffraction studies have been carried out at beam line X22A of the National Synchrotron Light Source (Brookhaven National Laboratory) [13].

By way of example, Fig. 2 shows two data sets displaying the intensity distributions in the η direction for the 26 nm ($\alpha = 0.15°$, $\beta = 32°$) and 88 nm ($\alpha = 0.02°$, $\beta = 42°$) LSMO films representing the thin and thick film situation (qualitatively the same intensity distribution is observed in the ξ direction). Our key observations are as follows: (a) The thin-film scenario [Fig. 2(a)] is dominated by satellite peaks which emerge with a constant in-plane momentum transfer $\Delta\eta$ implying a periodic height modulation $z(y)$ with a periodicity $2d$, $z(y) = z(y + 2d)$. The observed increase of the FWHM of the satellite peaks with $|\eta|$ discloses that this in-plane modulation is short ranged. (b) The thick film scenario [Fig. 2(b)] is dominated by twin peaks whose lateral η position increases linearly with L value. These twin peaks originate from individual TDs with (001) lattice planes tilted by an angle Φ_z with respect to the surface.

These two dominating structural motifs are illustrated in Fig. 3(a), the modulation structure from periodic twinning (left) and laterally coherent tilt domains (right). Notice that both motifs have the same origin: tilted lattice planes.

Also note that one observes satellite peaks, whenever a laterally correlated superstructure is present. Satellite peaks and twin peaks are simultaneously observed, especially well in the thick film [see red lines in Fig. 2(b)]. This is a strong indication that a 1D modulated structure of coherently connected TDs is formed (observed up to $t <$ 110 nm) [15]. The cubic STO favors [100] and [010] oriented domains equally as observed. Other satellite peaks as required for a 2D modulation have not been found at any Bragg reflection. In the 26 nm film the intensity contributions of the twin peaks are hidden under the satellite peaks and only "visible" in a quantitative intensity analysis. The central maximum ($\eta = 0$) originates both from the crystal truncation rod of the STO substrate (see sketch in Fig. 2) and from the film modulation structure [14]. As we show in

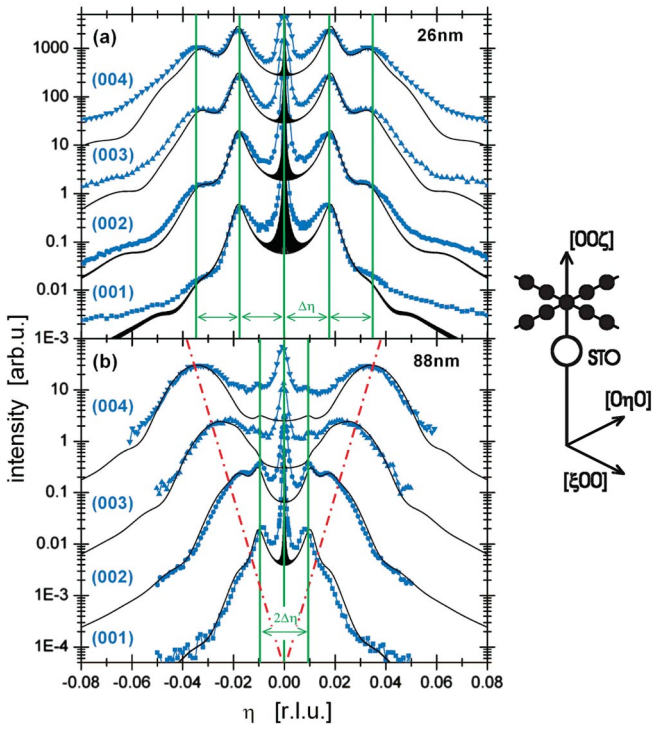

FIG. 2 (color). (a) Transverse scans of a 26 nm film at (001) to (004) at RT showing dominantly central peak and 1st and 2nd order satellite peaks (green solid lines), (b) transverse scans of a 88 nm film at (001) to (004) at RT showing dominantly twin peaks (red dashed lines as a guide to the eye) due to the tilted lattice planes. The numerically calculated intensity distribution of each reflection (solid curve) is superimposed using the microscopic matrix model. The sketch on the right shows the (00L) associated peak positions of the film (full circles) and the substrate (open circle), respectively.

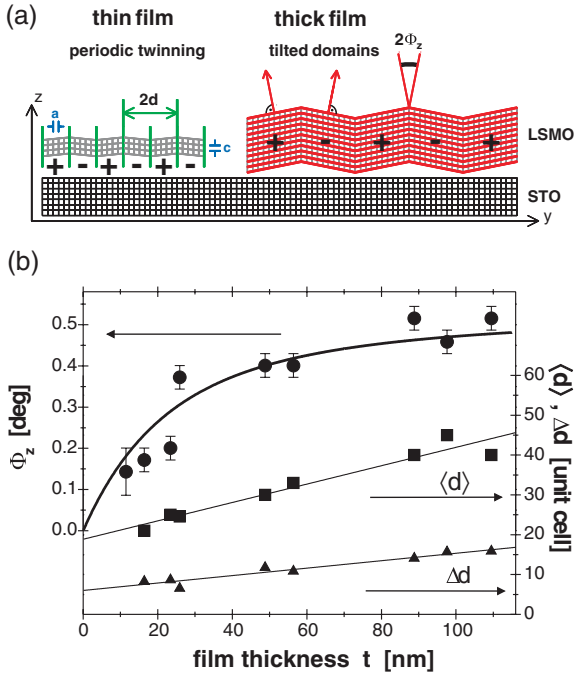

FIG. 3 (color). (a) Real space sketch to show which motifs of the film structure, grown in average pseudomorphically on top of a rigid, cubic substrate (STO) [6], are dominant in case of a thin (left) and a thick manganite film (right). The difference in variance of the TD length for the two cases is not illustrated in the picture. (b) Observed dependence of the twin angle Φ_z (circle) and TD length (mean value $\langle d\rangle$ (square) and its standard deviation Δd (triangle) upon film thickness t of the investigated manganite films.

what follows, the underlying structural changes that occur as the film thickness grows, are a continuous increase of the twin angle and of the size and the size distribution of the twin domains. The action of the continuous increase of the twin angle can directly be seen in Fig. 2: In the thick film limit the large twin angle displaces the TD intensity with the characteristic dispersion (red lines) well outside the modulation peaks (green lines). Because of the smaller twin angle in the thin-film limit the TD intensities are weak but become visible at large L underneath the 2nd order satellite peaks.

For a quantitative microscopic modeling of these strain relaxation phenomena we have developed a statistical matrix description which is closely connected with a model conceived for the description of surface faceting [16]. In our case of a 1D periodic arrangement of TDs, the film structure can be described by two types of domains ["+" and "−", see Fig. 3(a)]. Along z (film normal) they exhibit a distribution of twin angles Φ_z and Φ_x and domain sizes described by the average value $\langle d \rangle$ and the standard deviation Δd (for simplicity, all structural quantities are assumed to be constant). The twin angle Φ_x describes the tilting of the (100) film plane with respect to the substrate (100) lattice plane.

In a simple model, the manganite film can be considered as a linear chain of pseudocubic unit cells in the y direction, whereby all possible configurations of the chain have to be taken into account. The starting point for the calculation is the conditional probability $p_n^{\pm}$ of a domain change which depends on the domain type $(+, -)$ and on its strain energy (the index n describes the spatial deviation of the in-plane cell position with respect to the substrate lattice).

The observed x-ray intensity is then given by the sum over a rather straightforward correlation function $\langle F_0 F_m^* \rangle$ of two mth neighbored unit cells which can be cast into the closed matrix form

$$\langle F_0 F_m^* \rangle = \vec{A}^t \mathbf{M}^m \vec{B} e^{2\pi i \eta m} \tag{1}$$

with the x-ray structure factors $\vec{A}$ and $\vec{B}$ of the initial and final unit cell and the matrix $\mathbf{M}$, which contains all possible conditional probabilities $p_n^{\pm}$ of a domain change between two neighboring unit cells [17]. Figure 4 illustrates how the resulting domain structure is related with the stochastic quantity $p_n^{\pm}$. To fit our experimental results, we used the form $p_n^{\pm} = e^{(\pm n - N)/\sigma}$, where N $(-N)$ is the allowed maximum unit deviation from the average lattice. $\vec{A}$ and $\vec{B}$ are two-component vectors, e.g., $\vec{A} = (\vec{A}_+, \vec{A}_-)$, associated with the two types of twin domains $(+, -)$. Each component is a vector of the size $(2N + 1)$, whose elements n' are linked with the spatial deviation of the initial$(\vec{A})$/final$(\vec{B})$ unit cell. Their components read

$$(\vec{A}_{\pm})_{n'} = (\vec{B}_{\pm}^*)_{n'} P_{\pm}(N - n' + 1), \tag{2}$$

$$(\vec{B}_{\pm})_{n'} = F_{\pm}^* e^{2\pi i (N - n' + 1)(\zeta \tan\Phi_z + \xi \tan\Phi_x)}, \tag{3}$$

with the structure factors $F_{\pm}$ and with $P_{\pm}(n)$ as the probability to find the initial cell at deviation n, which is evaluated based on the conditional probability $p_n^{\pm}$ by using detailed balance [18].

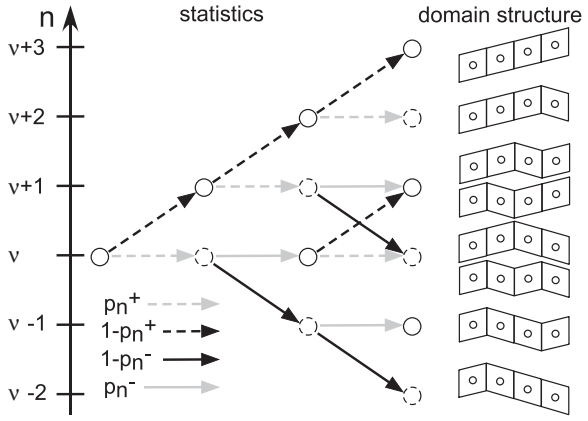

FIG. 4. Scheme of the statistical algorithm. The right-hand side shows the statistics tree for the first three steps and the left-hand side shows the resulting domain structure. n measures the deviation from the substrate horizon.

The relevant parameters describing the film structure versus film thickness are the average twin angle Φ_z, the average size $\langle d \rangle$ of the evolving domains, and its standard deviation Δd. While Φ_z directly enters the formalism via Eq. (3), $\langle d \rangle$ and Δd are nonlinearly related with N and σ. The final fits are shown as solid curves in Fig. 2 [19]. As can be seen, the fits describe all salient features in a self-consistent and quantitative way.

The obtained final results for $\langle d \rangle$, Δd, and Φ_z are summarized in Fig. 3(b) and show a rather interesting systematic dependence upon the film thickness t: The mean twin domain length $\langle d \rangle$ increases linearly from 20 unit cells (u.c.) for very thin films to 45 u.c. for 110 nm thick films, while the standard deviation Δd remains always about $\frac{1}{3}$ of $\langle d \rangle$. The mean twin angle Φ_z is close to zero for very thin films, but it increases monotonously with film thickness, until it saturates at $\Phi_z \approx 0.5°$ for films larger than 90 nm, which is most interestingly close to the single crystal twin angle of 0.6° for LSMO($\delta = 0.10$). Since the twin angle dispersion $\frac{\Delta \Phi_z}{\Delta t}$ as well as the number of domains (i.e., the inverse of the domain length) is highest for small film thicknesses, we conclude that films are strained strongest close to the STO interface. The observed saturation of the average twin angle with film thickness indicates that the strain relaxes, as one moves away from the substrate. The constant increase of the domain size shows that the films are not completely relaxed at the free surface.

Obviously, the MnO_6 octahedral tilt system alone cannot accommodate the strain well enough, instead, the low energy barrier for TD formation offers a new route for epitaxial strain minimization: the coherent periodic TD modulation. Similarly to the one in the (z-y) plane, there exists another coherent TD modulation with the same periodicity in the (x-y) plane, which is related to the twin angle Φ_x and which we have not shown here, since it does

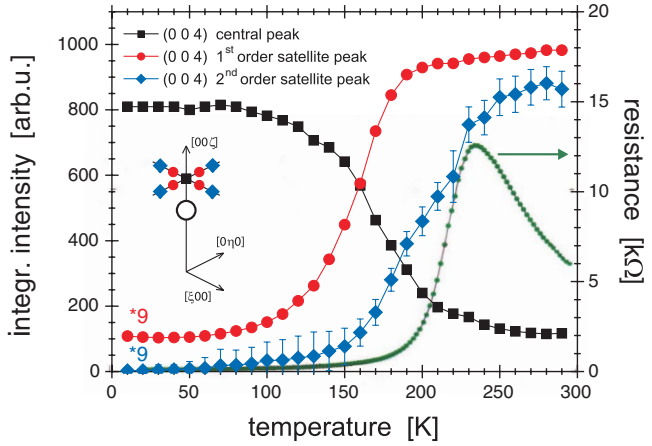

FIG. 5 (color). Temperature dependence of the structure [integrated intensity of the central peak and the 1st and 2nd order satellite peaks of the (004) Bragg reflection, whose η positions are indicated by vertical green lines in Fig. 2(a)] and transport of the 26 nm LSMO film. The inset shows the (00L) associated film (solid symbols) and substrate (open circle) peak positions.

not show up at (00L) peaks. Note that a periodic surface morphology to be responsible for our observations is clearly ruled out by the strong discrepancy in magnitude and direction of the surface miscut and the observed modulation periodicity [16,20] and as well as by the temperature dependence.

Figure 5 summarizes the measured temperature dependence of the (004) x-ray peak maxima associated with the 26 nm film (see Fig. 2) together with the recorded electrical resistance. We observe, that the satellite peaks disappear in accordance with resistivity below $T = 220$ K. This is the signature of a triclinic (related to $R\bar{3}c$) to monoclinic (related to $Pbnm$) phase transition in which Φ_z disappears abruptly. Φ_x survives, but does not contribute to the (004) intensity. Because of the strain gradient along z within the film, the structural phase transition is broadened between 100 and 220 K. This triclinic-monoclinic phase transition affects in turn strongly the octahedral MnO_6 tilt system [12] and, therefore, establishes a strong correlation between octahedral tilts and twin modulation waves.

Since a reduction of Φ_z could be compensated by the increase of an octahedral tilt, this would lead to an increase of the resistivity in contradiction to experiment, implying that the structural degrees of freedom in manganite films are not independent from Mn spin and charge state and orbital degrees of freedom. One finds a broadened metal-insulator phase transition around 230 K [2]. SQUID measurements on the same sample show a broadened paramagnetic-ferromagnetic transition between 110 and 215 K [21] (in bulk materials the $R\bar{3}c$ structure tends to be metallic). As thicker films gradually turn insulating at low temperatures [2], one might find the signature of an orbital-polaron lattice [22].

In summary, we have unraveled a novel strain relaxation phenomenon which exploits the delicate balance between MnO_6 octahedral tilts and the formation of twin modulation waves to adjust the manganite lattice parameter to the substrate. For thin films, a spinodal-type twin angle modulation evolves which progressively condensates into a twin domain structure as the film thickness increases. We showed by temperature-dependent x-ray and electronic transport experiments that this relaxation process is directly connected to the continuous metal-insulator transition in these films.

The authors acknowledge A. Rühm, J. Geck, D. Mannix, and G. Carbone for their help during experiments. The work performed at Brookhaven National Laboratory was supported by U.S. Department of Energy, Division of Materials Science, under Contract No. DE-AC02-98CH10886.

*Present address: Bruker AXS GmbH, Östl. Rheinbrückenstraße 50, 76181 Karlsruhe, Germany.
†Present address: Brock University, St. Catherines, Ontario L2S 3A1, Canada.

[1] A. J. Millis *et al.*, J. Appl. Phys. **83**, 1588 (1998).
[2] F. S. Razavi *et al.*, Appl. Phys. Lett. **76**, 155 (2000).
[3] P. M. Woodward, Acta Crystallogr. Sect. B **53**, 44 (1997).
[4] M. Déchamps *et al.*, Philos. Mag. A **80**, 119 (2000).
[5] A. J. Millis, in *Charge Density Waves in Solids*, edited by Y. Tokura, Advances in Condensed Matter Science Vol. 2 (Gordon and Breach, Amsterdam, 2000).
[6] O. I. Lebedev *et al.*, Philos. Mag. A **81**, 797 (2001).
[7] J. Geck *et al.*, Phys. Rev. B **69**, 104413 (2004).
[8] P. Kameli *et al.*, J. Magn. Magn. Mater. **283**, 305 (2004).
[9] A. Urushibara *et al.*, Phys. Rev. B **51**, 14 103 (1995).
[10] A. Heidemann *et al.*, Z. Phys. **258**, 429 (1973).
[11] Bulk LSMO with Sr doping $\delta = 0.10$ and $\delta = 0.125$ has at RT orthorhombic ($Pbnm$), the polycrystalline La-deficient LSMO rhombohedral ($R\bar{3}c$) symmetry.
[12] A. M. Glazer, Acta Crystallogr. Sect. A**31**, 756 (1975).
[13] Specular (00L) film Bragg reflections, but also reflections with nonzero in-plane components and superstructure peaks have been studied (see also [14]). Their intensity profiles did depend largely on the film thickness, but not on the chosen Sr doping.
[14] A. Vigliante *et al.*, Europhys. Lett. **54**, 619 (2001).
[15] The structure of much thicker films ($t > 200$ nm) also consists of TDs, however, with no evidence of a periodic arrangement.
[16] S. Pflanz *et al.*, Acta Crystallogr. Sect. A **48**, 716 (1992).
[17] Details will be published in a forthcoming paper.
[18] The spatial deviation of unit cells n from its equilibrium point reads $\Delta\vec{r}_n = na_s(\hat{x}\tan\Phi_x + \hat{z}\tan\Phi_z)$ with $n = -N, \ldots, N$.
[19] As we consider only one type of Bragg reflection in this Letter, (00L), we simplified the algorithm by assuming one atom per unit cell.
[20] V. Holý *et al.*, Phys. Rev. B **55**, 9960 (1997).
[21] Z.-H. Wang *et al.*, Phys. Rev. B **65**, 054411 (2002).
[22] J. Geck *et al.*, Phys. Rev. Lett. **95**, 236401 (2005).